`Int. J. Electrochem. Sci.*, 11**(2016)** 9902 – 9916, doi: 10.20964/2016.12.49

**International Journal of ELECTROCHEMICAL SCIENCE**
www.electrochemsci.org

# Electrochemical Synthesis, Characterization and Gas Sensing Properties of Hybrid Ppy/CS Coated ZnO Nanospheres

*Saeideh Ebrahimiasl*[1,*], *Azmi Zakaria*[2]

[1]Department of Chemistry, Ahar Branch, Islamic Azad University, Ahar, Iran;
[2]Institute of Advanced Technology, Universiti Putra Malaysia, 4340, UPM Serdang, Malaysia;
[*]E-mail: Ebrahimiasl.saeideh@yahoo.com

*Received:* 12 June 2016/ *Accepted:* 10 August 2016 / *Published:* 10 November 2016

Electrochemical deposition method was used to synthesis a new poly-pyrrole (Ppy), zinc oxide (ZnO) nanoparticles (NPs), and chitosan (CS) nanospheres. The Ppy/CS/ZnO film was analyzed for gas sensing properties. The morphology of Ppy/CS/ZnO electrodes was characterized by scanning electron microscopy (SEM), transmission electron microscopy (TEM). Chemical compositions of Ppy/CS/ZnO electrodes were characterized by energy dispersive X-ray analysis (EDX). A high selectivity and response towards hydrogen were realized with a ZnO NPs core and chitosan/Ppy shell hybrid nanospheres. Optimum sensing response was achieved with Ppy/CS nanospheres synthesized in the presence of 12 wt% ZnO NPs. The sensing response of fabricated sensor was proportional to the hydrogen gas concentration and exhibited a fast response over a wide dynamic range. The enhanced response originated from the sensing mechanism related with composition and morphology of deposited nanospheres.

**Keywords:** hybrid core-shell, nanobiocomposite, electrodeposition, hydrogen sensor

## 1. INTRODUCTION

The possibilities of combining the properties of organic and inorganic components in organic–inorganic nanocomposite, originate substantial attention to hybrid gas sensors. In which, the nanoparticles of metal oxide are embedded in an organic polymer matrix. They have many improved characteristics in comparison with most of the commercially available sensors, based on metal oxides. Hybrid heterojunctions are working on the barrier mechanism, in which no adsorption and desorption of oxygen for the detection of gas occur [1-2]. This mechanism of detection resulting in increased sensitivity towards toxic gases for the lower detectable limit, ease of operation and more efficiency [7-10]. Furthermore, the hybrid materials revealed more electrochemical and thermal properties to use in sensors [3].

So, the organic/inorganic hybrid materials with different combinations of the two components, PTP/$SnO_2$[4-5], PPy/$SnO_2$[6-7], PANI/$SnO_2$[8], PPy/$WO_3$[9], PTP/$WO_3$[10-11], PPy/ZnO [12], PANI/ZnO [13] and PPy-$Fe_2O_3$[14] have received more and more attentions and investigated for several toxic gas sensing performances. It revealed better gas sensing performances for hybrid sensors compared with the single component at low temperature. The zinc oxide (ZnO) together with PANI, an inorganic/organic hybrid structure shows a promising application in the gas sensors [15] It was found that PAni–$TiO_2$ and Ppy–ZnO hybrid materials had better selectivity and reversibility than PAni, Ppy and ZnO [3].

ZnO as a multifunctional semiconducting metal oxides, have been utilized as a most promising materials for biosensing and gas sensing because of its unusual properties. High surface area, chemical stability, high nontoxicity, catalytic efficiency, and strong adsorption ability (high isoelectric point ~9.5) are its pivotal properties [16-18]. But generally, metal oxide sensors with high operation temperatures and low selectivity to gases are not attractive for a wide range of applications.

Conducing polymers attracted considerable attention in the application as a resistive type sensor, because of high sensitivity, short response time, room temperature operation, facile fabrication, controllable electrical conductivity, low energy optical transitions, low ionization potential and high electron affinity and good mechanical properties [19-20]. Their noticeable conductometric response turned them as a potential sensing element in the detection of toxic gases and volatile organic compounds (VOC)[21] including ammonia [8-9, 22-27], hydrazine [28], nitric oxide[29-30], and methanol [31]. Among conductive polymers, polypyrrole with alternative single and double bonds and broad π-electron conjugation is a suitable material as the active layers in gas sensors [20]. When it is exposed to electron-donating gases, an electronic interaction between the gaseous component and the positive charge along the Ppy chains causes a redox reaction and variation of electronic density [9, 22-27].

To improve the structural and physical properties of Ppy, extensive researches have been done to construct its composite. In this regard, chitosan (CS) as a biocompatible, biodegradable, nontoxic, and low-cost biopolymer, the most widely used to prepare Ppy/CS composite. This combination increase the mechanical, antibacterial, electrochemical, and biocompatible properties of the resulting products [32]. The Ppy/CS composite introduced with different applications such as waste water treatments, separation membranes, drug delivery systems, biosensors and gas sensors [33].

Therefore, a new generation of the conductive composites of Ppy/CS has been developed with high galvanostatic cycling stability, high thermal stability and high sensitivity for use in nanofibrous membrane, flexible energy devices and gas sensors or biosensors respectively [32].

Thus, a combination of polypyrrole to reduce response time and room temperature operation with a chitosan to increase mechanical stability and electrochemical properties assemble the high performance sensor. Furthermore, presence of ZnO NP in Ppy/CS matrix, increase surface area and sensitivity of composite. The barrier mechanism of adsorption for Ppy/CS/ZnO organic-inorganic sensor brings better selectivity and reversibility for synthesized sensor. Thus performance of the new formulated sensor is expected could be improved by combining the advantage of the all constituents.

## 2. EXPERIMENT

### *2.1. Materials and methods*

The pyrrole monomer (Fluka St Gallen, Switzerland) was distilled prior to use and stored at 4°C. ZnO nanopowder, acetic acid (Sigma-Aldrich) was used without further purification. Indium tin oxide (ITO) glass and sodium salt of p-toluene sulfonic acid (p-TS) were supplied by Sigma-Aldrich Co. (St Louis, MO, USA) and were used as substrate and dopant respectively. CS powder (98.0%) supplied by Acros Organics (Fair Lawn, NJ, USA), was solvate in 1% acetic acid solution and stirred continuously with a magnetic stirrer for 1 hour. After completely dissolution of CS powder in the solution, the mixture was left at the laboratory for 5 hours.

A well-dispersed suspension of ZnO NPs with different weight ratios (3, 6, 9, 12 and 15wt%) prepared by dissolution in double distilled water (DDW) and sonicated for 30 minutes to avoid the disaggregation of NPs. The suspension pours to the CS solution under vigorous stirring for 30 minutes. A potentiostat (Elchema, Potsdam, NY, USA, Model: PS 605) was used for electrochemical deposition of Ppy/CS/ZnO NBC film on the ITO glass surface. The film deposition was performed in a solution with the concentrations of 0.3 M Ppy, 0.1 M p-TS, and 0.7% (w/v) CS and at a constant voltage of 1.2 volts (vs standard calomel electrode [SCE]). The electrochemical deposition was conducted in 1 hour and 30 minutes to obtain a desired thickness. The film was rinsed thoroughly with DDW, and dried in an oven at 45°C for 2 hours.

### *2.2. Apparatus*

All electrochemical deposition was carried out using a potentiostat (Model: PS 605). In the electrochemical cell three-electrode was arranged with an ITO glass working electrode, a carbon rod counter electrode and saturated calomel reference electrode (Metrohm, Switzerland).

Chemical composition of composite was characterized by XRD-6000 instrument (Shimadzu, Osaka, Japan), at a scan speed of 4° per minute with Cu Kα1 radiation (λ=1.54060 Å) operating at 40 kV and 40 mA.

Scanning electron microscope (SEM) LEO 1455 (JEOL, Eching, München, Germany) attached to EDX (Energy dispersive X-ray) were performed to analysis the morphology and composition of the film. TEM images were acquired with Hitachi H-7100 (Japan) transmission electron microscope.

### *2.3. Evaluation of gas sensitivity*

The gas sensor unit was specially designed to test the gas sensing ability of heterojunction. The I-V characteristics of the sample were examined by making front Ag (silver conductive paste) contact and back ITO glass contact to a heterojunction sample having area 1 cm × 1 cm. The gas sensor unit was specially designed with homemade sealed glass vacuum chamber of 2 L volume having gas inlet/outlet ports.

All measurements were performed at room temperature. Current-Voltage (I-V) characteristic on the sensor were obtained using a source meter (Keithley Model 2400). The forward biased I-V

characteristics of fabricated sensor, placed in the test chamber, were recorded before and after exposure of gases for different concentrations. The maximum current change arose at a fixed potential was noted from I-V characteristics and used to calculate the gas response (sensitivity) by the following equation:

$$S(\%) = \frac{I_a - I_g}{I_a} \times 100 = \frac{\Delta I}{I_a} \times 100 \qquad (1)$$

where $I_a$ is the electrical currents in air and $I_g$ is the electrical currents upon exposure to gases.

Gas volume measurement unit contain glass bottle comprising double distilled water connected to a pipette (measuring unit of the volume) with gas inlet and outlet pipe. The desired amount of gas volume is injected in the gas chamber by the rate of 10 ml per second which is prefilled with air.

## 3. RESULTS AND DISCUSSION

### *3.1. Characterization*

Fig. 1 shows the XRD patterns of ZnO nanopowder , Ppy/CS and Ppy/CS/ZnO composite with different concentration of ZnO NPs (6% and 9% wt). A broad scattering peak was observed for Ppy/CS composite, which connoted its highly amorphous structure and arising from the Ppy chains close to the interplanar Vander-Waals distance for aromatic groups [34-35]. The diffraction patterns for Ppy/CS/ZnO composite exhibited the peaks of ZnO phase (JCPDS file 075–1533) corresponding to (101) and (100) crystallographic planes. The pattern demonstrated that intensity of the characteristic peaks of ZnO NPs increase by increase in ZnO concentration up to 9 wt%, and peaks become sharper. In the Ppy/CS–ZnO nanocomposites, the broad peak of Ppy/CS and the assigned to the ZnO phase was observed without any appreciable change in peak positions or widths.

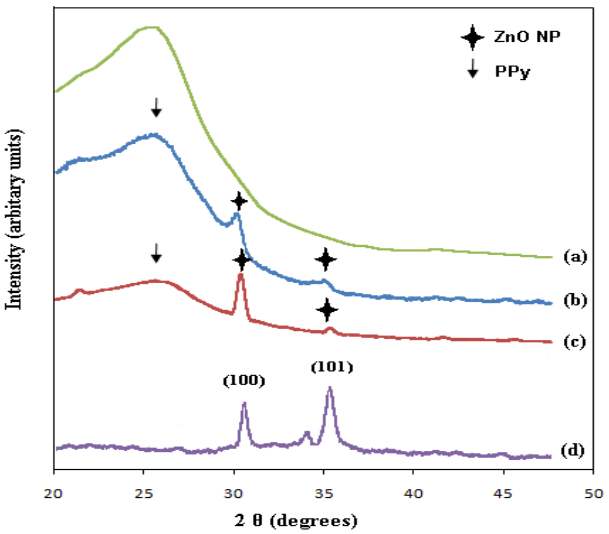


**Figure 1.** The XRD patterns of (a) Ppy/CS, (b) Ppy/CS/ZnO 6 wt%, (c) Ppy/CS/ZnO 9 wt% composite films and (d) pure ZnO nanopowders. Abreviation**:** wt%, weight percentage

Fig. 2 represents SEM images of Ppy/CS synthesized with the addition of 12 wt% ZnO NPs by weight. The smooth film has been obtained for Ppy/CS sample, whereas Ppy/CS nanospheres were formed with the addition of ZnO NPs. The synthesis of polymers in the presence of structure directing molecules which act as soft templates gives better uniformity in the morphology of nanostructure [36-39]. The amount of ZnO as additive, during polymerization of composite, has played a pivotal role in controlling the morphology of Ppy/CS and by the addition of 12 wt% ZnO, good quality nanospheres were formed [40]. The average diameter of these nanospheres is about 180 nm. The decrease in ZnO content increased cross linked morphology of Ppy/CS composite and due to smoothing of the film.

Because of the porous structure of Ppy/CS/ZnO nanoshperes presented in Fig. 2, promoted gas sensing, catalytic application and adsorption of different biological molecules through the film surface and consequently superior sensitivity and response can be surmised [41-42]. SEM micrograph confirms the homogeneous film formation of Ppy with CS and ZnO NPs and lack of any phase discrete.

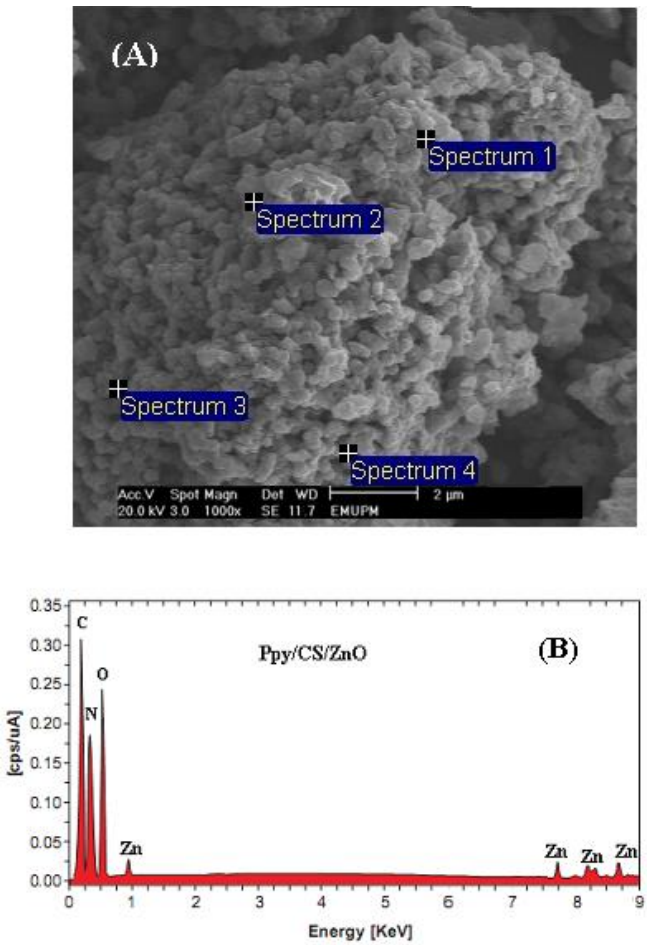


**Figure 2.** Scanning electron microscopy images (A) and energy-dispersive X-ray fluorescence spectra (B) of Ppy/ CS/ZnO (12 wt%). Abbreviations: cps, counts per second; Ppy, polypyrrole; CS, chitosan; wt%, weight percentage; ZnO, zinc oxide.

The energy-dispersive X-ray fluorescence (EDXRF) spectra of the Ppy/CS/ZnO nanospheres are presented in Fig. 2B. The peaks related to binding energies of carbon and nitrogen in the Ppy structure was observed at around 0.3 and 0.4 keV. The peak at around 0.5 keV is related to binding energy of oxygen which can be related to the ZnO structural oxygen and oxidation form of pyrrole. The peaks related to $Zn^{2+}$ elements was observed around 0.9, 7.8, 8.3, and 8.8 keV. The intensity of the peaks is in compliance with elemental composition and stoichiometric ratio of elements in Ppy/CS/ZnO nanospheres.

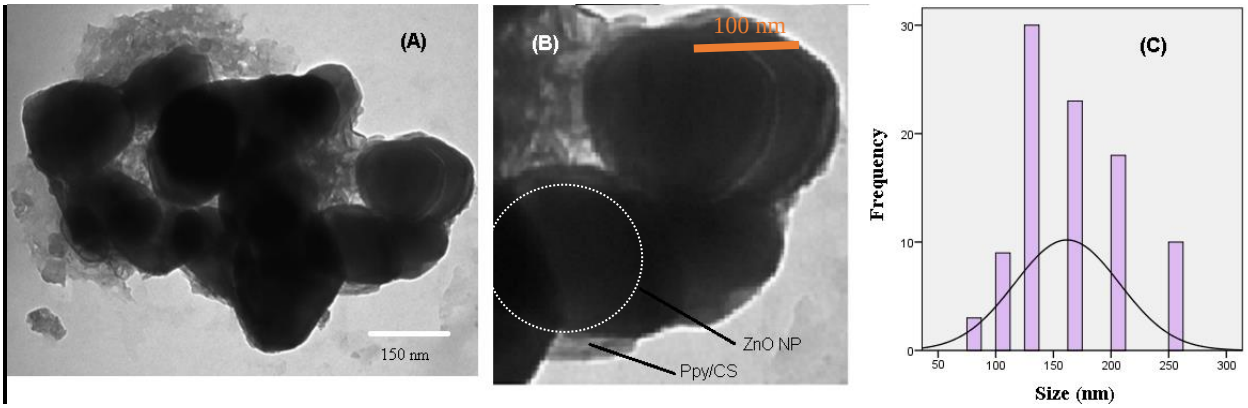


**Figure 3.** TEM images of Ppy/CS/ZnO composite at low (A) and high (B) magnification. ZnO particles embedded inside the Ppy/CS matrix (C), normalized frequency of size distribution in composite (D) respectively.

Table 1 shows the elemental analysis in different area of scan in the surface of the Ppy/CS/ZnO film. The result was presented by weight percentage of every element.

**Table 1.** Weight percentage of every element in EDX analysis at different area of scan in the surface of Ppy/CS/ZnO film.

| Spectrum | C | O | N | Zn | Total |
|---|---|---|---|---|---|
| **Spectrum 1** | 47.85 | 18.70 | 21.08 | 12.36 | 100.00 |
| **Spectrum 2** | 51.07 | 29.43 | 13.83 | 5.66 | 100.00 |
| **Spectrum 3** | 53.24 | 33.26 | 10.11 | 3.40 | 100.00 |
| **Spectrum 4** | 31.73 | 29.68 | 15.71 | 22.88 | 100.00 |
| **Mean** | 45.97 | 27.76 | 15.18 | 11.07 | 100.00 |
| **Std. deviation** | 9.75 | 6.29 | 4.57 | 8.74 | |

Abreviation: Std, standard deviation

The maximum and minimum percentage of the elements and the mean value with standard deviation are presented for different parts of the film. It is observed that elemental composition of the film has confirmed molecular weight ratio of the Ppy/CS/ZnO. Therefore, the EDXRF spectrum of Ppy/CS/ZnO NBCs according to the presence of elemental compounds with their expected ratio without any impurity peaks.

The detailed morphology and structure of the samples were further characterized and analyzed by TEM. The typical TEM image (Fig. 3A & B) shows the core/shell nature of the product resulting from the electro-polymerization of Ppy/CS and ZnO NPs. Well-defined particles were readily observed with light contrast Ppy/CS shells and dark contrast cores of ZnO. The ZnO@Ppy/CS core/shell structure with well sphere morphology was achieved. The normalized frequency of size distribution is presented in Fig. 3C. The mean size of 180 nm was observed for the synthesized Ppy/CS/ZnO nanospheres.

### *3.2. Gas sensing studies*

#### *3.2.1. Selectivity studies*

The typical I-V characteristic of Ppy/CS/ZnO heterojunction for optimized film thickness (0.8 µm) is shown in Fig. 4.The I-V characteristic shows rectifying behavior indicating the formation of good quality diode.

The forward biased voltage characteristics of Ppy/CS/ZnO nanosphere for different gases at room temperature in voltage range of 0 to +2.5 V are presented at Fig. 5. It is shows the I-V characteristic before exposure to the gas (in air) and after exposure to the $CO_2$, $N_2$ and $H_2$ gases at 500 ppm concentration and 6 wt% of ZnO NPs. It is observed that the maximum change in current density is observed for $H_2$ as compared to $CO_2$ and $N_2$. Fig. 6 shows the sensitivity bar diagram of NBCs towards $H_2$ (16.03%), $CO_2$ (8.77%) and $N_2$ (3.51%) in 6 wt% of the ZnO NPs. The Ppy/CS/Zn NBC showed more selectivity for $H_2$ compared to $N_2$ and $CO_2$.

The synergistic combination of advantages of PPy and CS and ZnO NPs expected to enhance sensitivity of the Ppy/CS/ZnO nanospheres compared with pristine CS or PPy. Increase of surface to volume ratio in Ppy/CS/ZnO nanospheres compare with pristine PPy and CS provides more active sites of PPy for gas adsorption [43]. Ppy film based sensor produced lower as well as slower response, and suffered from severe noise (long-time instability and irreversibility) compared with Ppy/CS/ZnO nanospheres[44]. The signal- to- noise ratio (S/N) of pristine Ppy and Ppy/CS/ZnO were measured by:

$$S/N = P_s/P_n \qquad (2)$$

Were $P_s$ is the power of signal ratio and $P_n$ is the power of the noise ratio. The result of S/N ratio of pristine Ppy (S/N=0.13) was much higher than that of Ppy/CS/ZnO (S/N=$10^{-4}$). Therefore, the nanosphere structure of Ppy/CS/ZnO composite increase the accessibility of more active sites for adsorption of gases and improved performance of synthesized gas sensor. Similar phenomena were

observed in previous research [24], where multi/single walled carbon nano-tubes were coated with electrically conducting PPy fabrics.

Gas sensing mechanism of organic-inorganic heterojunctions has been differentially expressed. Heterojunctions are diodes which can be employed as simple gas sensor due to its potential barrier dependent model. The principle of formation of heterojunction barrier in air ambient and their interrupt on exposure to the gasses is the mechanism used to detection of gasses [15].

Another explanation to the response of conductive polymers to toxic gases is also according to the redox reaction. Chitosan is a good $\pi$-electron donors, so when a composite film of chitosan (CS) and conducting polymer exposed to electron acceptor gases, electrons will transfer from CS to gases and an increase in structural holes of chitosan. At a p-type conducting composite, this phenomena enhanced the doping level as well as the electric conductance of the conducting composite [22-24, 45]. Therefore dopants type and levels, have an effect on the physical and chemical properties of composite.

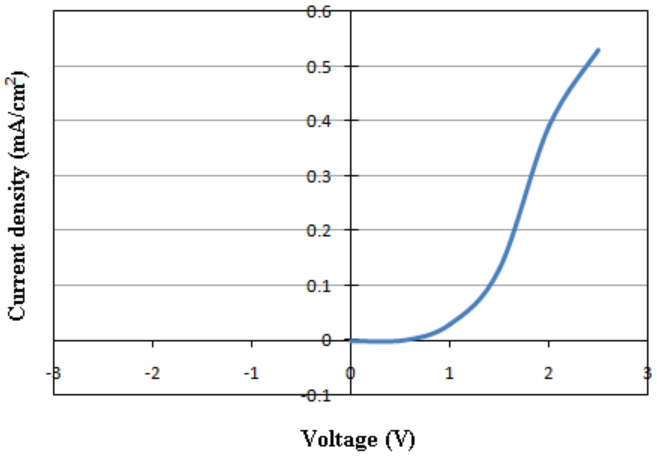


**Figure 4.** Typical I-V characteristics of Ppy/CS/ZnO NBC

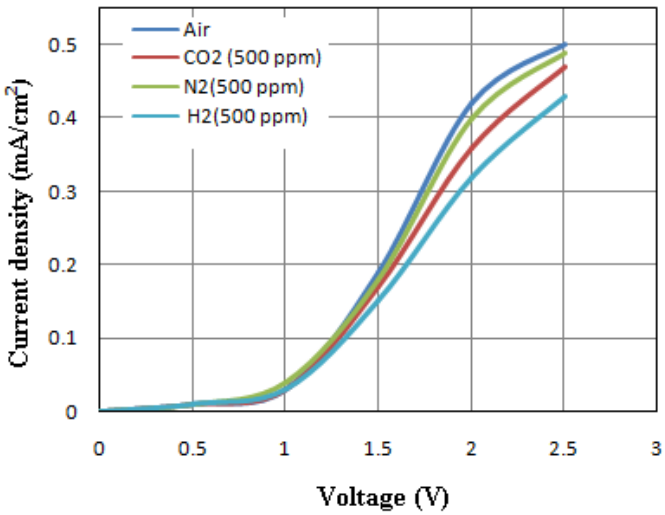


**Figure 5.** Forward biased I-V characteristics of Ppy/CS/ZnO NBC in the voltage range of 0 to +2.5 volt and at a concentration of 500 ppm for various gases.

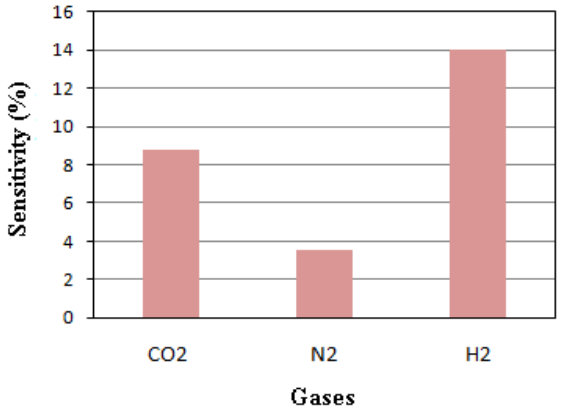


**Figure 6.** Selectivity bar diagram of Ppy/CS/ZnO NBC in the presence of different gases at 500 ppm $H_2$ concentration.

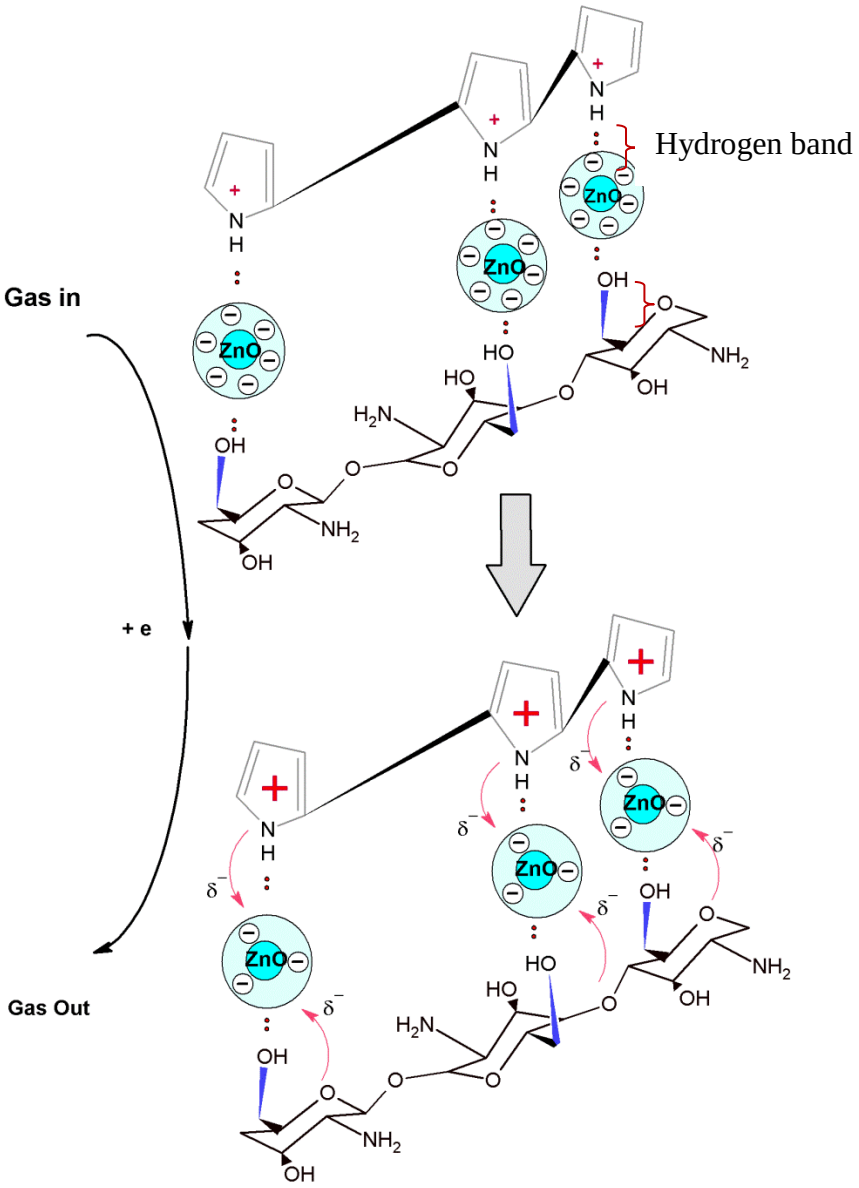


**Figure 7.** Schematic gas sensing mechanism of the Ppy/CS/ZnO NBC.

Conducting polymers doped with small inorganic ions showed a resistance increase to electron donating gas [46]. ZnO NP with a partial negative charge in the surface of the particles acts as an electron donating material and increase the resistance of the synthesized NBC and resistivity to electron donating gas. The result demonstrated that the Ppy/CS/ZnO nanocomposite reveal more sensitivity towards electron acceptor gases ($H_2$). The barrier mechanism of gas detection for hybrid composite material (Ppy/CS and ZnO NP) presented fast response and recovery time. Schematic diagram of $H_2$ detection based on the results is presented in Fig 7 for the synthesized Ppy/CS/ZnO composite.

### *3.2.2. Gas Sensitivity*

Fig. 8 represents forward biased I–V characteristic and sensitivity plots of Ppy/CS/ZnO NBC at room temperature and in the absence and presence of different concentrations of $H_2$ (250, 500 and 1000 ppm) and 6 %wt of ZnO NPs. The figures show the I–V characteristics in air ambient and in $H_2$ for the concentration succession of 250 to 1000 ppm. A shift is occurred in the I–V characteristics after exposure of the gas. The response of the Ppy/CS/ZnO NBC to the gas shows a concentration-dependent behavior.

The forward current radically decreased by exposure of the Ppy/CS/ZnO NBC to $H_2$ and subsequently increases in concentration of $H_2$ up to 1000 ppm (Fig. 8). The decrease in forward current has been ascribed to the decrease in charge carrier concentration and change in work function of the NBC by gas molecules exposure to the surface of the film [15]. This observation is in good agreement with previous reports of Ppy-based sensors. A detectable concentration for Ppy/CS/ZnO sensor, significantly is lower than other Ppy-based sensors [27]. Different methods were used for detection of $H_2$, in which the good sensitivity, fast response and recovery time for room temperature Ppy/CS/ZnO composite is noticeable [28].

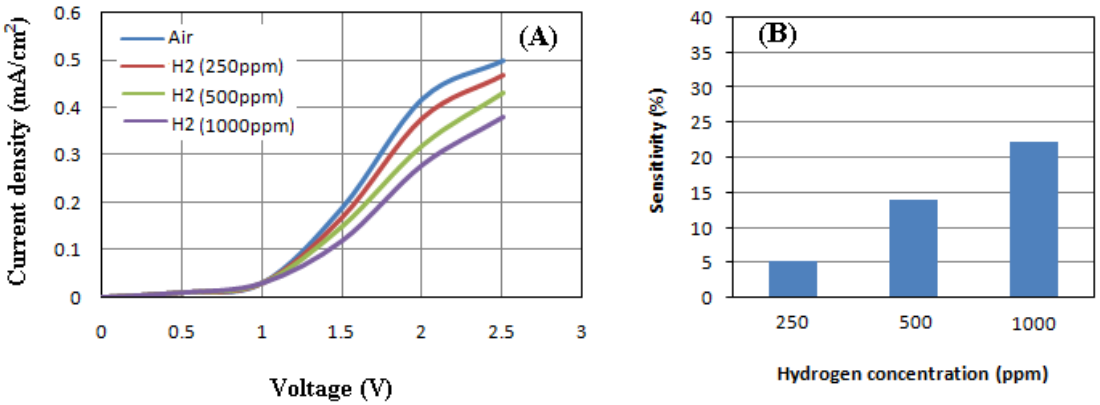


**Figure 8.** Forward biased I-V characteristics (A) and sensitivity (B) of Ppy/CS/ZnO Nanocomposite at various concentration of Hydrogen.

*3.2.3. Sensitivity by percentage of nano ZnO*

On the whole, the composition, conjugation and chain lengths, level and type of doping, compactness of the sample, etc can affect the conductivity and sensitivity of the nanocomposites. For all the reported sensitivity values, the senisitivity value of Ppy-based nanocomposites was higher than that of pure Ppy [47-48].

The gas sensitivity test of Ppy/CS/ZnO NBC [Ppy/CS–ZnO (3%), Ppy/CS–ZnO (6%), Ppy/CS–ZnO (9%), Ppy/CS–ZnO (12%) and Ppy/CS–ZnO (15%)] to $H_2$ was carried out at room temperature (Fig. 9). The results demonstrated that the sensitivity of Ppy/CS/ZnO NBC with different ZnO weight ratios were 10.6%, 14%, 14.1%, 18.3%, 20% and 19%, respectively. It was indicated that Ppy/CS/ZnO NBC had better selectivity and higher sensitivity than Ppy, Ppy/CS and ZnO at room temperature. It is also observed that the addition of chitosan to Ppy increased its sensitivity and decrease the weight ratio of ZnO NPs subsequently [19]. It was also revealed that Ppy/CS/ZnO (12%) nanocomposite has maximum sensitivity to 500 ppm of $H_2$ at room temperature. This can be related to change in the morphology of the film in different concentration of ZnO NP, which increases the surface area and the approachability of more active sites for adsorption of gases. This improved performance of Ppy/CS/ZnO nanospheres as expected is attributed to the lower background noise and the increased surface area. [9, 22-24].

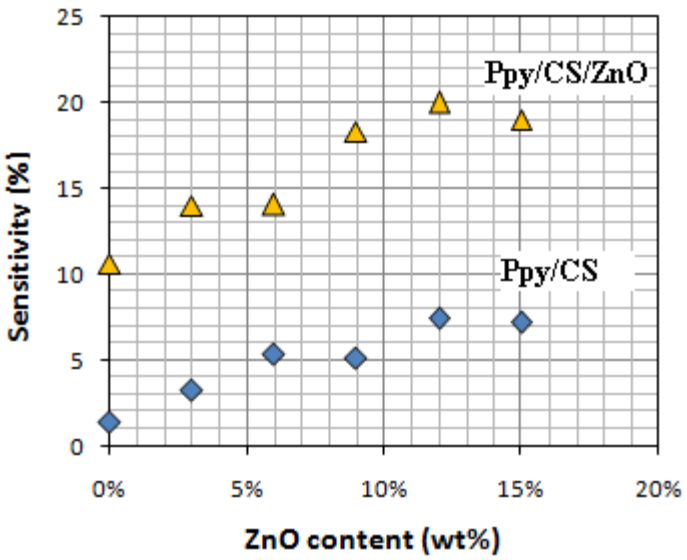


**Figure 9.** The sensitivity of Ppy/CS and Ppy/CS/ZnO (3, 6, 9, 12 and 15 %wt) nanocomposite in 500 ppm of $H_2$ at room temperature.
Abreviation: wt%, weight percentage.

*3.2.4. Dynamic response*

Fig. 10 shows the dynamic variation of gas response in different concentration of gas flow (250, 500 and 1000 ppm) versus time at ZnO NP (12 %wt). It is reveal that the sensitivity of the heterojunction reached its maximum in short time upon exposure of $H_2$ (500 ppm) and dropped rapidly

when the gas was removed from testing atmosphere. This evinced good response (75s) and recovery time (50 s) for the sensor which are shorter than those of pristine Ppy or Ppy composite sensors [49]. This could be due to the fact that the morphology of Ppy/CS/ZnO nanosphere translates to more surface area for gases to diffuse into. Furthermore, the gas molecules permeated into Ppy/CS/ZnO composite complete adsorption and desorption process very fast due to the reversible binding and electron transfer from NBC to the gas [21, 23, 50-51].

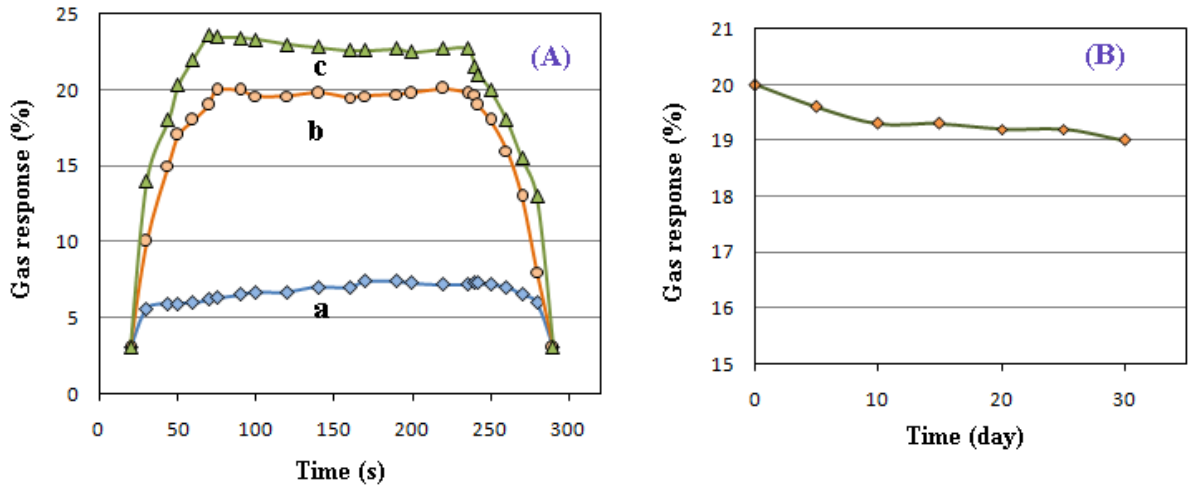


**Figure 10.** The gas response (%) vs. time (s) plot of the Ppy/CS/ZnO nanospheres at voltage of +2.5 volt and 12wt% of ZnO NP and at a different concentration of hydrogen (A) stability studies of composite in 30 days (B).

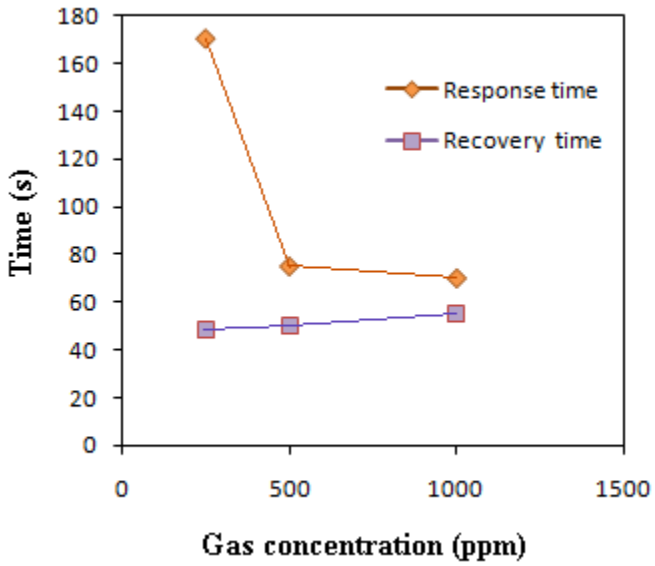


**Figure 11.** Sensing characteristics (sensor response time, recovery time) of the Ppy/CS/ZnO nanospheres at room temperature and different concentration of hydrogen.

Response and recovery time period was measured by detecting I-V characteristics in forward biased region for different $H_2$ concentrations. The response and recovery time variation by the $H_2$ concentration was illustrated in Fig. 11 for the Ppy/CS/ZnO nanosphere. The result demonstrated that,

response time decreases from 170 to 70 s by increases $H_2$ concentration from 250 to 1000 ppm. The recovery time periods of the heterojunction increases from 48 to 55 s by increases in $H_2$ flow concentration up to 1000 ppm. The complete reversibility and short recovery time have been obtained which is the advantage of using chitosan biopolymer in sensor structure. Similar phenomena have not been observed for most PPy-based sensors [22-24, 26, 52].

## 4. CONCLUSION

Organic-inorganic Ppy/CS/ZnO core-shell heterojunction was synthesized by electro-deposition method on ITO glass substrate. The heterojunction exhibited a linear dependence of sensor response and ZnO NPs concentrations at room temperature. XRD and EDX analysis showed the successfully formation of PPy/CS/ZnO hybrid nanocomposites. The intensity of the peaks, increased as the ZnO NPs concentration increase. EDX results confirm the expected stoichiometric ratio of Ppy, CS and ZnO NPs. SEM and TEM analysis demonstrated that ZnO NPs are well incorporated in over the polymer matrix and exhibited porous and granular morphology suitable for gas sensing applications. Gas sensing properties of Ppy/CS/ZnO nanospheres was studied against $H_2$ in room temperature. The highly porous structure of ZnO-coated Ppy/CS nanospheres and ultrathin layer of film offer a high surface area for the free access of gases to diffuse. This reduces the gas diffusion resistance, leading to excellent sensitivity and fast response/recovery. The optimal mixing ratio was 12 %wt of ZnO NP, which yielded maximum sensitivity over the whole range of tested $H_2$ concentration, with a response and recovery time of about 75 and 50 s, respectively. The results herein demonstrated the potential application of Ppy/CS/ZnO NBC in the fabrication of high-performance gas sensors.

ACKNOWLEDGEMENTS
The authors would like to thank Ahar Branch, Islamic Azad University for the financial support of this research, which is based on a research project contract.

## References

1. K. Hikita, M. Miyayama, H. Yanagida, *Journal of the American Ceramic Society*., 78 (1995) 865-73.
2. Z. Ling, C. Leach, R. Freer, *Journal of the European Ceramic Society*., 23 (2003) 1881-91.
3. P. Kannusamy, T. Sivalingam, *Polymer Degradation and Stability*., 98 (2013) 988-96.
4. F. Kong, Y. Wang, J. Zhang, H. Xia, B. Zhu, Y. Wang, S. Wang, S. Wu. *Materials Science and Engineering: B*, 150 (2008) 6-11.
5. M. Xu, J. Zhang, S. Wang, X. Guo, H. Xia, Y. Wang, S. Zhang, W. Huang, S. Wu., *Sensors and Actuators* B: Chemical., 146 (2010) 8-13.
6. J. Zhang, S. Wang, M. Xu, Y. Wang, H. Xia, S. Zhang, X. Guo, S. Wu. *The Journal of Physical Chemistry C*, 113 (2009) 1662-5.
7. G.L.-N.W. Shu-Rong, L.P.Z.Y.-Q. ZHANG, S.-M.W. Shi-Hua. *Chinese Journal of Inorganic*

*Chemistry*, 7 (2005) 005.
8. L. Geng, Y. Zhao, X. Huang, S. Wang, S. Zhang, S. Wu. *Sensors and Actuators B: Chemical*. 120 (2007) 568-72.
9. L. Geng, X. Huang, Y. Zhao, P. Li, S. Wang, S. Zhang, S. Wu. *Solid-state Electronics*. 50 (2006) 723-6.
10. J. Huang, Y. Kang, T. Yang, Y. Wang, S. Wang. *Journal of Natural Gas Chemistry*. 20 (2011) 403-7.
11. X.-z. Guo, Y.-f. Kang, T.-l. Yang, S.-r. Wang. *Transactions of Nonferrous Metals Society of China*. 22 (2012) 380-5.
12. L. Geng, Y. Zhao, X. Huang, S. Wang, S. Zhang, W. Huang, S. Wu. *Synthetic Metals*. 156 (2006) 1078-82.
13. J. Huang, T. Yang, Y. Kang, Y. Wang, S. Wang. *Journal of Natural Gas Chemistry*. 20 (2011) 515-9.
14. L. Geng, S. Wang, Y. Zhao, P. Li, S. Zhang, W. Huang, S. Wu. *Materials Chemistry and Physics.* 99 (2006) 15-9.
15. D. Dhawale, D. Dubal, A. More, T. Gujar, C. Lokhande. *Sensors and Actuators B: Chemical.* 147 (2010) 488-94.
16. S. Singh, S.K. Arya, P. Pandey, B. Malhotra, S. Saha, K. Sreenivas, V. Gupta. *Applied Physics Letters*. 91 (2007) 063901-3.
17. A. Wei, X.W. Sun, J. Wang, Y. Lei, X. Cai, C.M. Li, Z. L. Dong, W. Hoang. *Applied Physics Letters.* 89 (2006) 123902-3.
18. J. Wang, X.W. Sun, A. Wei, Y. Lei, X. Cai, C.M. Li, Z. L. Dong. *Applied Physics Letters.* 88 (2006) 233106-3.
19. M.A. Chougule, D.S. Dalavi, S. Mali, P.S. Patil, A.V. Moholkar, G.L. Agawane, J. H. Kim, S. Sashwati, V. Patil.. *Measurement*. 45 (2012) 1989-96.
20. H. Bai, G. Shi. *Sensors*, 7 (2007) 267-307.
21. Q. Ameer, S.B. Adeloju. *Sensors and Actuators B: Chemical*. 106 (2005) 541-52.
22. R. Gangopadhyay, A. De. *Sensors and Actuators B: Chemical*. 77 (2001) 326-9.
23. S.C. Hernandez, D. Chaudhuri, W. Chen, N.V. Myung, A. *Electroanalysis*. 19 (2007) 2125-30.
24. J. Jang, J. Bae. *Sensors and Actuators B: Chemical.* 122 (2007) 7-13.
25. D. Kincal, A. Kumar, A.D. Child, J.R. Reynolds. *Synthetic Metals*. 92 (1998) 53-6.
26. M. Penza, E. Milella, M. Alba, A. Quirini, L. Vasanelli. *Sensors and Actuators B: Chemical*. 40 (1997) 205-9.
27. H. Yoon, M. Chang, J. Jang. *The Journal of Physical Chemistry. B*, 110 (2006) 14074-7.
28. R. Aitout, A. Belgaid, L. Makhloufi, B. Saidani. *Reactive and Functional Polymers*. 66 (2006) 373-7.
29. B.J. Holliday, T.B. Stanford, T.M. Swager. *Chemistry of materials*. 18 (2006) 5649-51.
30. W.C.A. Koh, M.A. Rahman, E.S. Choe, D.K. Lee, Y.-B. Shim. *Biosensors and Bioelectronics*. 23 (2008) 1374-81.
31. H. Hammache, L. Makhloufi, B. Saidani. *Synthetic Metals*. 123 (2001) 515-22.
32. S. Ebrahimiasl, A. Zakaria, A. Kassim, S.N. Basri. *International journal of nanomedicine*. 10 (2015) 217.
33. A. Bouvree, J.-F. Feller, M. Castro, Y. Grohens, M. Rinaudo. *Sensors and Actuators B: Chemical*. 138 (2009) 138-47.
34. G. Mitchell, A. Geri. *Journal of Physics D: Applied Physics*. 20 (1987) 1346.
35. A. Kassim, H. Block, F.J. Davis, G.R. Mitchell. *J Mater Chem*. 2 (1992) 987-8.
36. H. Yin, J. Yang. *Materials Letters*. 65 (2011) 850-3.
37. Y. Zhu, J. Li, M. Wan, L. Jiang. Polymer. 49 (2008) 3419-23.
38. D. Zhou, Y. Li, J. Wang, P. Xu, X. Han. *Materials Letters*. 65 (2011) 3601-4.
39. L. Zhang, L. Zhang, M. Wan. *European Polymer Journal*. 44 (2008) 2040-5.

40. V. Talwar, O. Singh, R.C. Singh. *Sensors and Actuators B: Chemical*. 191 (2014) 276-82.
41. M. Ghosh, A. Barman, A. Das, A. Meikap, S. De, S. Chatterjee. *Journal of applied physics*. 83 (1998) 4230-5.
42. E. Håkansson, T. Lin, H. Wang, A. Kaynak. *Synthetic Metals*. 156 (2006) 1194-202.
43. K.H. An, S.Y. Jeong, H.R. Hwang, Y.H. Lee. *Advanced Materials*. 16 (2004) 1005-9.
44. B. Kondratowicz, R. Narayanaswamy, K. Persaud. Sensors and Actuators B: Chemical. 74 (2001) 138-44.
45. Y. Wang, W. Jia, T. Strout, A. Schempf, H. Zhang, L. Baikun. C. Junhong, Y. Lei. *Electroanalysis*. 21 (2009) 1432-8.
46. V. Chabukswar, S. Pethkar, A.A. Athawale. *Sensors and Actuators B: Chemical*. 77 (2001) 657-63.
47. S. Patil, M. Chougule, S. Pawar, S. Sen, A. Moholkar, J. Kim, V. Patil. *Sensors & Transducers* (1726-5479), 134 (2011).
48. Q. Wan, Q. Li, Y. Chen, T.-H. Wang, X. He, J. Li, C. Lin. *Applied Physics Letters*. 84 (2004) 3654-6.
49. L. Jiang, H.-K. Jun, Y.-S. Hoh, J.-O. Lim, D.-D. Lee, J.-S. Huh. *Sensors and Actuators B: Chemical*. 105 (2005) 132-7.
50. G. Gustafsson, I. Lundström, B. Liedberg, C. Wu, O. Inganäs, O. Wennerström. *Synthetic Metals.* 31 (1989) 163-79.
51. C. Lin, B. Hwang, C. Lee. *Materials Chemistry and Physics*. 55 (1998) 139-44.
52. E. Kriván, C. Visy, R. Dobay, G. Harsányi, O. Berkesi. *Electroanalysis*. 12 (2000) 1195-200.